

Supplementary Information

**Edge-grafting carbon nitride with aromatic rings for high-
efficient charge separation and enhanced photocatalytic
hydrogen evolution**

Zhang-Jie Liu Wei-De Zhang* and Yu-Xiang Yu

School of Chemistry and Chemical Engineering, South China University of
Technology, 381 Wushan Road, Guangzhou, 510641, People's Republic of China

*Corresponding author. E-mail address: zhangwd@scut.edu.cn (W. D. Zhang).

Reagents

Urea ($\text{CH}_4\text{N}_2\text{O}$, $\geq 99\%$) was purchased from Guangdong Guanghua Sci-Tech Co. Ltd. (Guangzhou, China). 2-Aminoquinoline (QL, $>97\%$), β -Naphthylamine (NA, 98%) and triethanolamine (TEOA, 98.0%) were obtained from Aladdin Chemistry Co. Ltd. (Shanghai, China). All chemicals in this text were used without further purification. Deionized (DI) water was produced from a pure water system (GWA-UN, Beijing, China).

Characterization

X-ray diffraction (XRD) was carried out on a Bruker D8 Advance powder X-ray diffractometer with a $\text{Cu K}\alpha$ radiation source. Fourier transform infrared (FT-IR, Shimadzu IR Affinity-1, Japan) spectra were recorded by mixing the samples with KBr and pressed to pellets. Raman spectra were collected on a Horiba Jobin Yvon LabRAM HR800. ^{13}C solid-state nuclear magnetic resonance (NMR) spectra were measured on the Bruker AVANCE III 600M NMR spectrometer. Morphologies of the prepared samples were observed with a Zeiss Merlin SEM at an acceleration voltage of 5 kV, and a JEM-2100F TEM at an acceleration voltage of 200 kV with a Bruker X-Flash 5030 T X-ray energy dispersive spectrometer. UV-vis diffuse reflectance spectra (DRS) were taken on a Hitachi U-3010 UV-visible diffuse reflectance spectrophotometer using BaSO_4 as a reflectance. Photoluminescence (PL) spectra were collected on Hitachi F-4500 fluorescence spectrophotometer with excitation wavelength at 360 nm. Thermogravimetric analysis was performed on a Q500 SDT TA ING TGA under nitrogen atmosphere with a ramping rate of $10\text{ }^\circ\text{C}/\text{min}$. X-ray photoelectron spectroscopy (XPS) was implemented on a Thermo ESCALAB 250Xi electron spectrometer using 150 W Al $\text{K}\alpha$ radiation as an exciting source.

Photocatalytic H_2 evolution

Photocatalytic HER experiments were carried out in a seal circulatory system

with a light source ($\lambda > 420$ nm) which is provided by a 300 W Xe lamp (PLS-SXE 300/300UV, Beijing Perfectlight Technology Co. Ltd., China). The average light intensity was adjusted to $100 \text{ mW}\cdot\text{cm}^{-2}$ determined by a PL-MW2000 spectroradiometer. In brief, 50 mg catalyst was uniformly dispersed in an aqueous solution (100 mL) containing triethanolamine (TEOA, 10 vol%) as a sacrificial electron donor. After sonicating for 30 min, the suspension was transferred to a reaction cell together with 3 ml (3 wt%) H_2PtCl_6 as a cocatalyst precursor. The reaction system was evacuated to vacuum before irradiation. During the reaction, the generated hydrogen was determined by gas chromatography (GC7806, Beijing Weipuxin Analytical Instruments Co. Ltd, China) adopting nitrogen as a carrier. The apparent quantum efficiency (AQE) of the samples were measured under the same photocatalytic reaction conditions under monochrome light irradiation with wavelengths of 380, 400, 450, 500, and 550 nm, respectively. The intensity of the light with wavelength of 450 nm was $2.04 \text{ mW}\cdot\text{cm}^{-2}$, which was determined by a light intensity meter.

Photoelectrochemical measurement

The photocurrent response curves (I-t), Mott-Schottky plots, linear sweep voltammograms (LSV) and electrochemical impedance spectra (EIS) were measured on an electrochemical workstation (CHI 660C, Shanghai Chenhua, China), with Pt electrode as a counter electrode, saturated Ag/AgCl electrode as a reference electrode, and a working electrode. The working electrode was prepared as follows: 30 mg sample and 3 mg ethyl cellulose were evenly dispersed in anhydrous ethanol under sonication. Then, 50 μL of the above suspension was dropped onto a $1 \text{ cm}\times 1 \text{ cm}$ FTO glass followed by drying at $60 \text{ }^\circ\text{C}$ overnight. The light source was a 300 W PLS-300/300UV Xe lamp ($\lambda \geq 420$ nm), and a phosphate buffer solution with pH 6.5 was adopted as the electrolyte. Electrochemical impedance spectroscopy (EIS) plots were taken at the corresponding open circuit potential with frequency ranging from 10^{-2} to 10^6 Hz in 0.01 M $\text{K}_3\text{Fe}(\text{CN})_6/\text{K}_4\text{Fe}(\text{CN})_6$ (1:1) solution in the dark.

ICP-OES analysis

The as-prepared samples (10 mg) were added in 10 mL freshly prepared aqua regia (HCl/HNO₃ with a volume ratio of 3:1), followed by sonication for 24 h. After that, the samples were diluted to 40 mL and filtered out all solid by syringe-driven filters. The supernatant solutions were analyzed by an inductively coupled plasma spectrometer.

DFT calculation

To simulate the HOMO and LUMO of UCN, UCN-NA and UCN-QL, DFT calculation was performed using a Gaussian 09 program. All calculations are based on B3LYP function and the 6-31 G (d, p) basis sets. The smallest unit constructed and optimized by Chem3D was used as the calculation model.

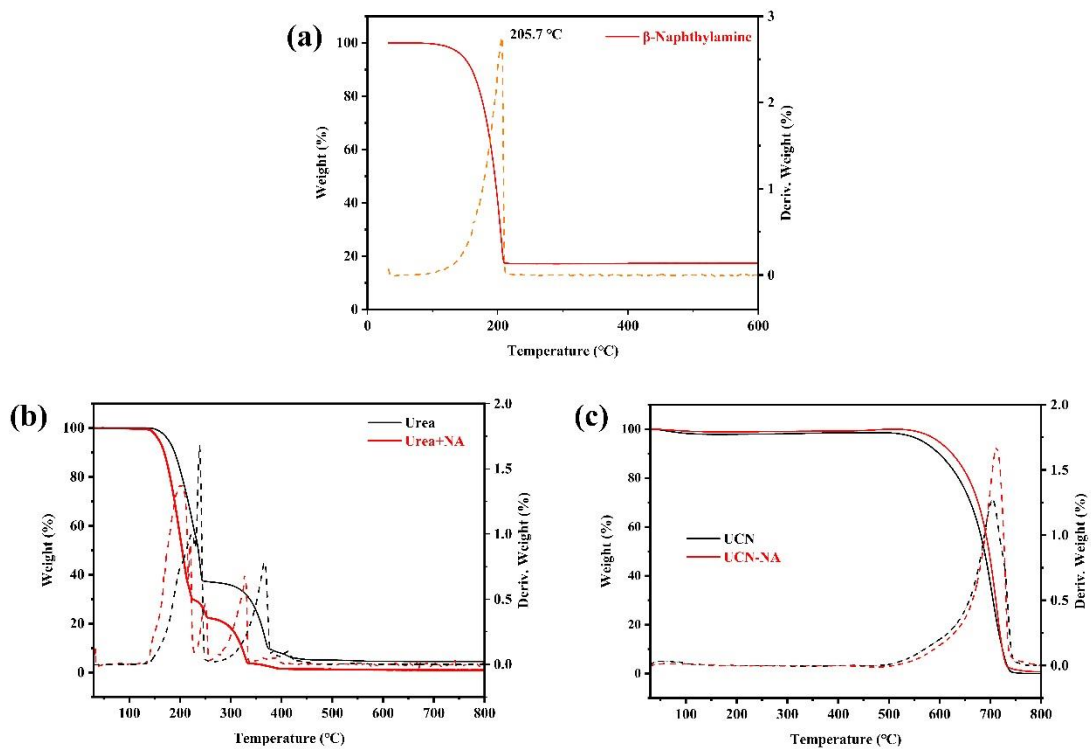


Fig. S1. TGA-DTG curves of (a) β -naphthylamine, (b) urea and the mixture of urea and NA, (c) UCN and UCN-NA.

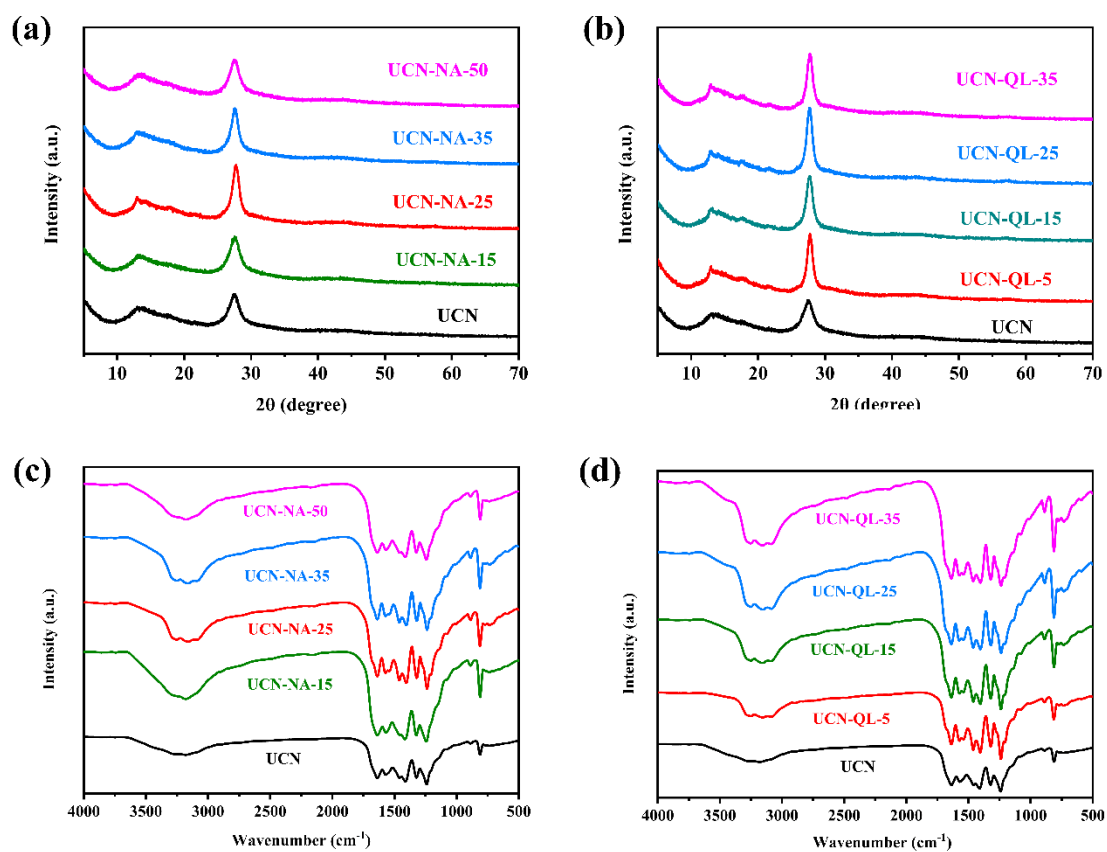


Fig. S2. XRD patterns of (a) UCN-NA, (b) UCN-QL with different contents of NA or QL; FT-IR spectra of (a) UCN-NA, (b) UCN-QL with different contents of NA or QL.

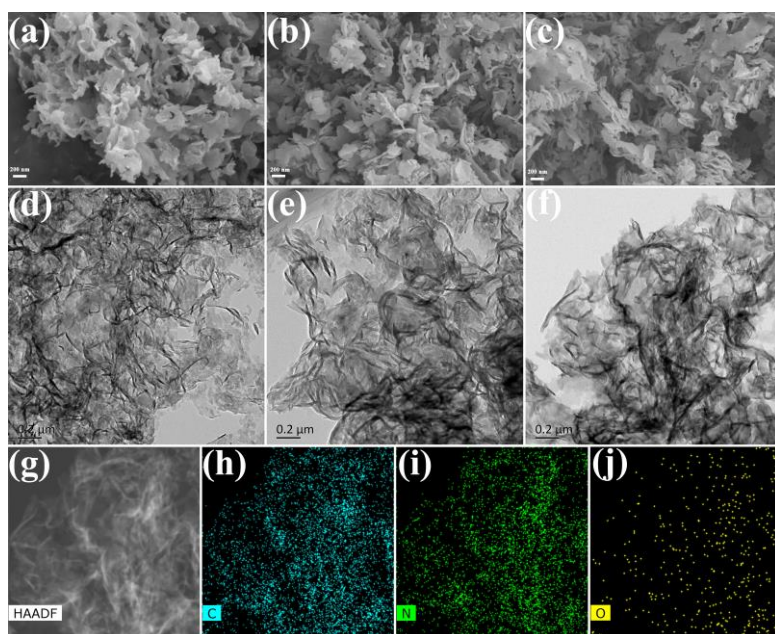


Fig. S3. (a-c) SEM images, (d-f) TEM images of UCN, UCN-NA and UCN-QL. (g) HAADF-STEM of UCN-QL and (h-j) the corresponding elemental mappings of C, N and O. The selected area in (h-j) is the same as (g).

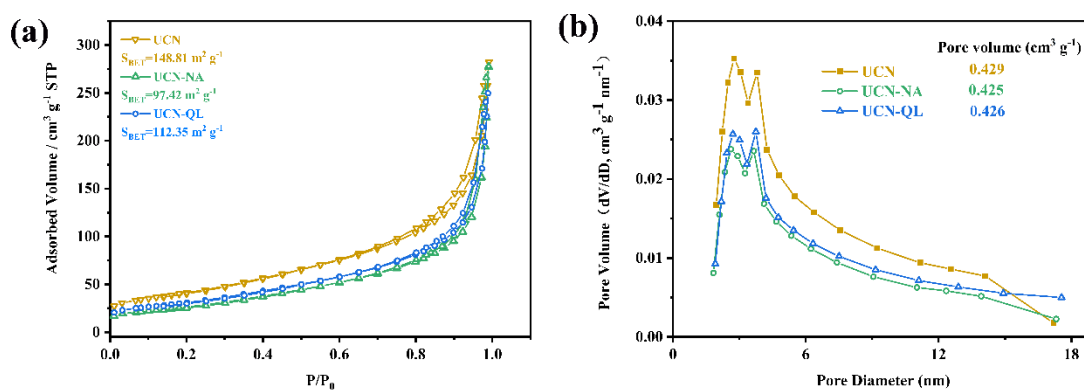


Fig. S4. (a) Nitrogen adsorption-desorption isotherms and (b) pore size distribution curves of UCN, UCN-NA and UCN-QL.

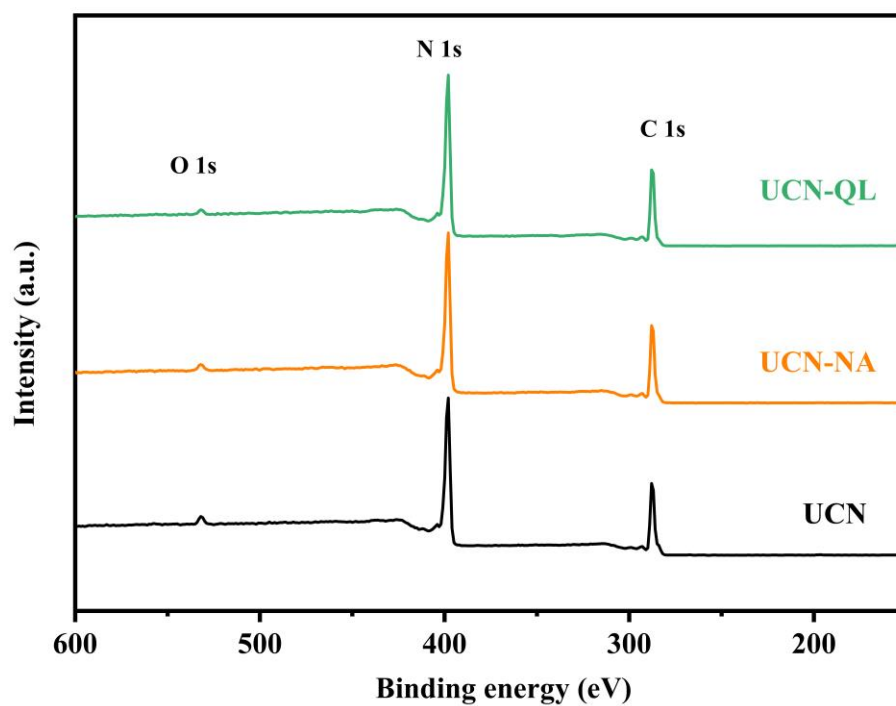


Fig. S5. XPS survey spectra of UCN, UCN-NA and UCN-QL.

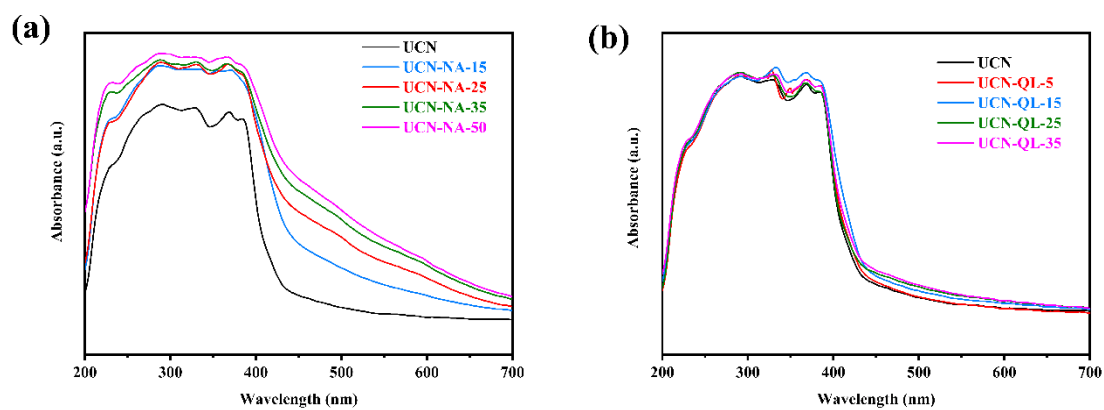


Fig. S6. UV-vis spectra of (a) UCN-NA, (b) UCN-QL with different contents of NA or QL.

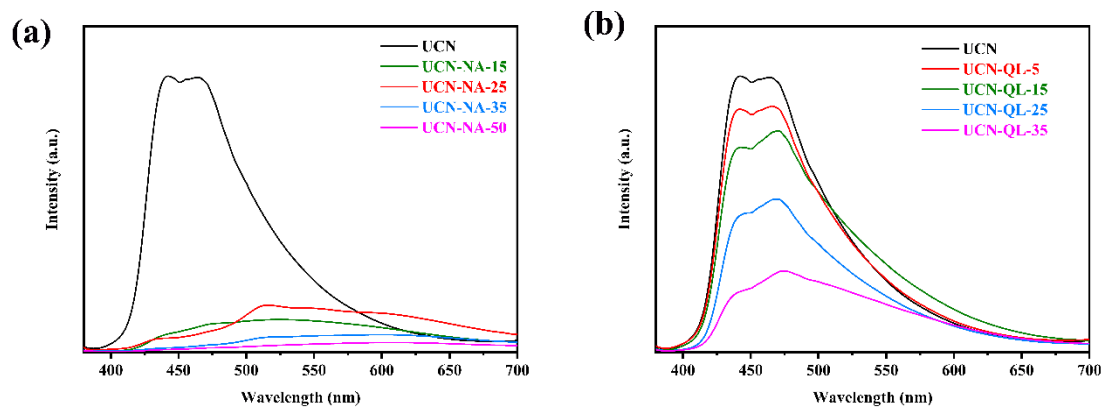


Fig. S7. PL spectra of (a) UCN-NA, and (b) UCN-QL with different contents of NA or QL.

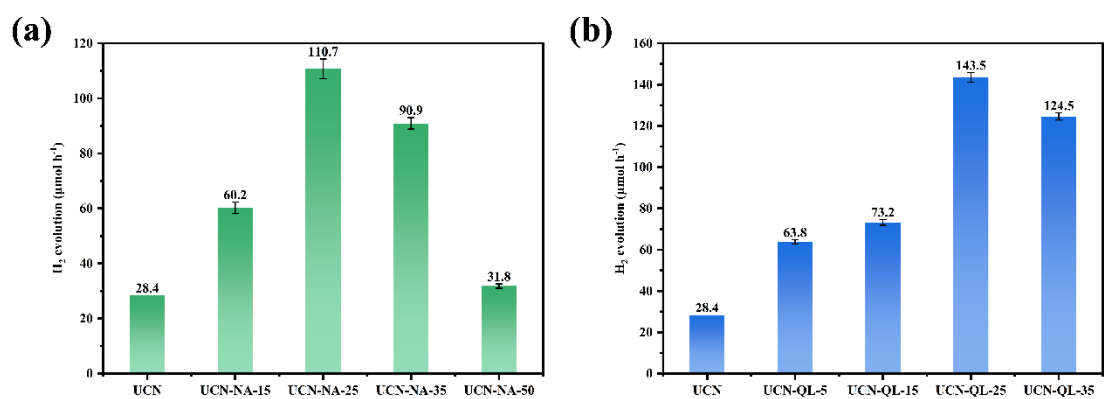


Fig. S8. Photocatalytic H₂ evolution rates over (a) UCN-NA-X and (b) UCN-QL-X.

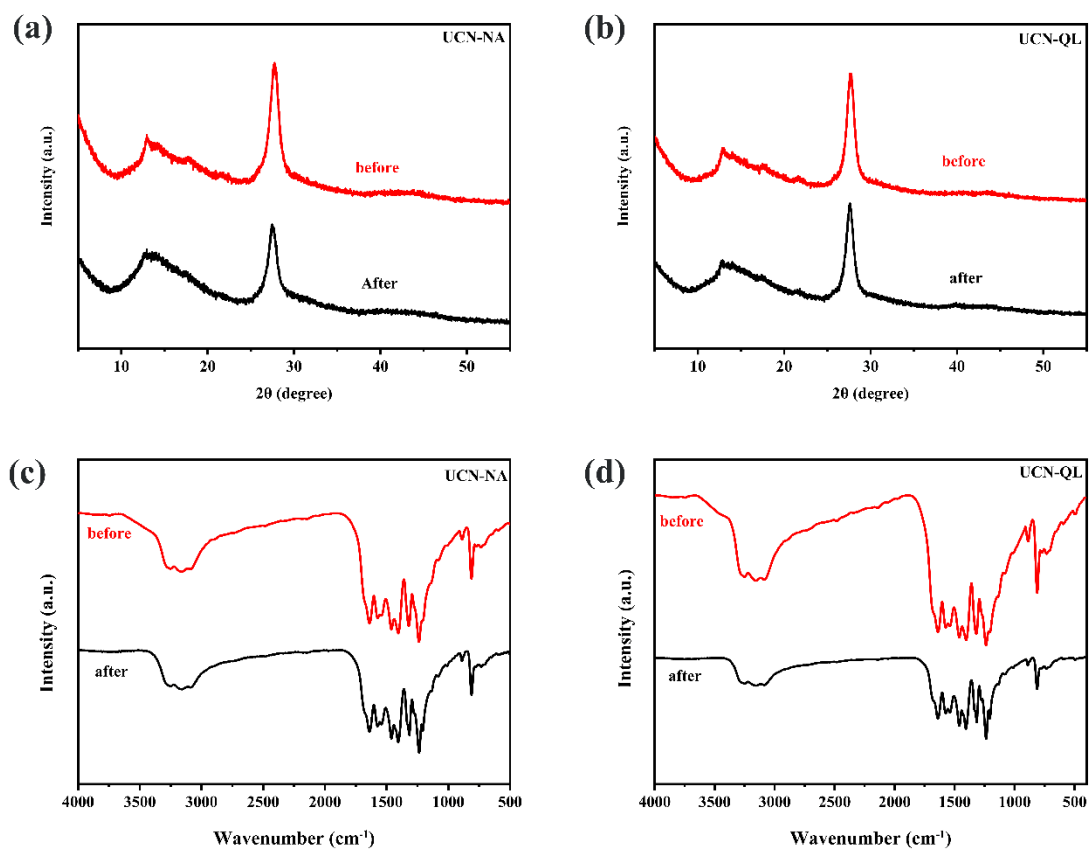


Fig. S9. XRD patterns of (a) UCN-NA and (b) UCN-QL before and after reaction; FT-IR spectra of (c) UCN-NA and (d) UCN-QL before and after photocatalytic reaction.

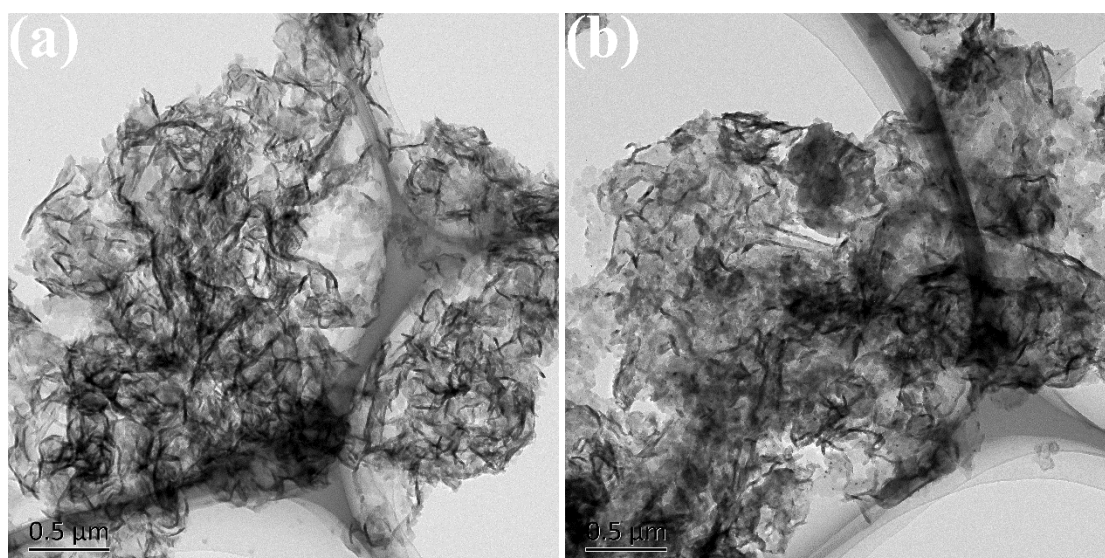


Fig. S10. TEM images of UCN-QL (a) before and (b) after photocatalytic reaction.

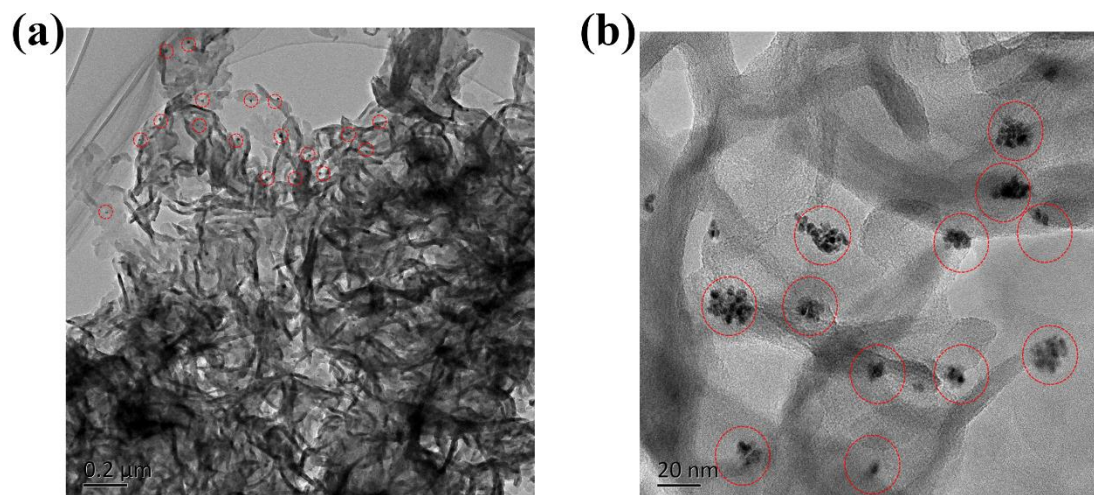


Fig. S11. TEM images of UCN-QL loaded with Pt nanoparticles.

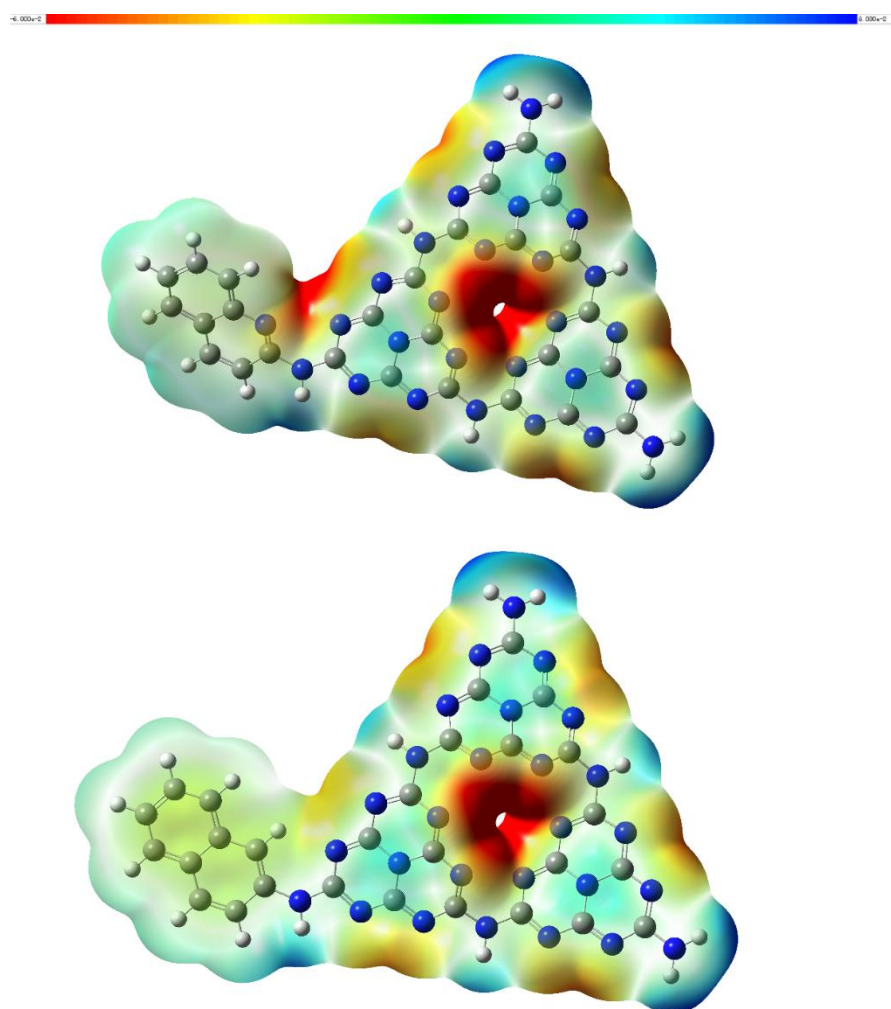


Fig. S12. Electrostatic potential (ESP) maps of UCN-NA model (Top) and UCN-QL model (bottom). Red corresponds to a region of the lower potential, while blue corresponds to the higher potential.

Table S1. Proportions of nitrogen species from N 1s spectra of UCN, UCN-NA and UCN-QL (obtained from the peak area of the fitted curve).

Sample	N (C=N-C) area (%)	N (N-(C)₃) area (%)	N (-NH_x) area (%)	π excitation area(%)
UCN	67.51	17.94	10.93	3.62
UCN-NA	75.22	11.35	7.99	5.44
UCN-QL	71.40	22.21	2.80	3.59

Table S2. Comparison of photocatalytic performance over molecular doping CN-based catalysts reported.

Catalyst	Dosage (mg)	Light source	Reaction Conditions	Hydrogen Evolution Rate ($\mu\text{mol h}^{-1} \text{g}^{-1}$)	Ref.
UCN-QL-25	50	300 W Xe lamp, $\lambda > 420 \text{ nm}$	3 wt% of Pt; Aqueous TEOA solution (10 vol%)	2870	<i>This work</i>
UCN-NA₁₀₀	50	300 W Xe lamp, $\lambda > 420 \text{ nm}$	3 wt% of Pt; Aqueous TEOA solution (10 vol%)	2042	¹
H₃BTC/CN	20	300 W Xe lamp, $\lambda > 420 \text{ nm}$	3 wt% of Pt; Aqueous TEOA solution (10 vol%)	301	²
CN-TA₂₀	10	300 W Xe lamp, $\lambda > 420 \text{ nm}$	0.5 wt% of Pt; Aqueous TEOA solution (10 vol%)	890	³
CN-DNP0.1	50	300 W Xe lamp, $\lambda > 420 \text{ nm}$	2.5 wt% of Pt; Aqueous TEOA solution (10 vol%)	2262.4	⁴
NP-CN_{0.2}	50	300 W Xe lamp, $\lambda > 420 \text{ nm}$	3 wt% of Pt; Aqueous TEA solution (20 vol%)	2791.4	⁵
CNU_{0.075}	50	300 W Xe lamp, $\lambda > 420 \text{ nm}$	3 wt% of Pt; Aqueous TEA solution (20 vol%)	1003.94	⁶
SCN-BTH	50	300 W Xe lamp, $\lambda > 420 \text{ nm}$	1 wt% of Pt; Aqueous TEA solution (10 vol%)	3950	⁷
PCN-BPT₁₅	50	300 W Xe lamp, $\lambda > 420 \text{ nm}$	3 wt% of Pt; Aqueous TEOA solution (20 vol%)	2500	⁸
CN-DAP₃₆	30	5 W LED light	0.2 wt% of Pt; Aqueous TEOA solution (10 vol%)	2800	⁹
CHD-g-C₃N₄	50	300 W Xe lamp, $\lambda > 420 \text{ nm}$	1.5 wt% of Pt; Aqueous TEOA	522	¹⁰

CN-40	25	300 W Xe lamp, $\lambda > 420$ nm	3 wt% of Pt; Aqueous TEOA solution (10 vol%)	1210.3	¹¹
CGCN-2	50	300 W Xe lamp, $\lambda > 420$ nm	3 wt% of Pt; Aqueous TEOA solution (10 vol%)	1024	¹²

References

1. K. Li, M. Sun and W.-D. Zhang, *Carbon*, 2018, **134**, 134-144.
2. D. Yuan, X. Chen, Z. Li, C. Fang, J. Ding, H. Wan and G. Guan, *Applied Surface Science*, 2021, **569**, 151089.
3. X. Lin, X. Hou, L. Cui, S. Zhao, H. Bi, H. Du and Y. Yuan, *Journal of Materials Science & Technology*, 2021, **65**, 164-170.
4. Y. Jiao, J. Qin, Y. Li, J. Wang, Z. He and Z. Li, *J Colloid Interface Sci*, 2022, **616**, 691-700.
5. C. Li, T. Zhou, M. Yan, S. Cheng, Y. Wang, J. Sun, G. Chen and H. Dong, *Inorganic Chemistry Frontiers*, 2022, **9**, 60-69.
6. Y. Huang, D. Li, Z. Fang, R. Chen, B. Luo and W. Shi, *Applied Catalysis B: Environmental*, 2019, **254**, 128-134.
7. Z. Liu, J. Zhang, Y. Wan, J. Chen, Y. Zhou, J. Zhang, G. Wang and R. Wang, *Chemical Engineering Journal*, 2022, **430**, 132725.
8. X. Zhou, B. Xu, J. Zhang, Q. Zhao, C. Li, H. Dong, X. Wang and J. Yang, *International Journal of Hydrogen Energy*, 2021, **46**, 38299-38309.
9. Z. Li, S. Zhou, Q. Yang, Z. Zhang and X. Fang, *The Journal of Physical Chemistry C*, 2019, **123**, 2228-2237.
10. J. Wu, C. Li, H. Dong, H. Zhang, J. Han, L. Wang, S. Yu and Y. Wang, *Renewable Energy*, 2020, **157**, 660-669.
11. Y. Liu, S. Zhao, C. Zhang, J. Fang, L. Xie, Y. Zhou and S. Zhuo, *Carbon*, 2021, **182**, 287-296.
12. P. Deng, H. Li, Z. Wang and Y. Hou, *Applied Surface Science*, 2020, **504**, 144454.